A New Oxoanion: $[IO_4]^{3-}$ Containing I(V) with a Stereochemically Active Lone-Pair in the Silver Uranyl Iodate Tetraoxoiodate(V), $Ag_4(UO_2)_4(IO_3)_2(IO_4)_2O_2$

Amanda C. Bean,[†] Charles F. Campana,[‡] Ohyun Kwon,[†] and Thomas E. Albrecht-Schmitt*,[†]

Contribution from the Department of Chemistry, Auburn University, Auburn, Alabama 36849, and Bruker AXS, 5465 East Cheryl Parkway, Madison, Wisconsin 53711

Received May 15, 2001

Abstract: The hydrothermal reaction of elemental Ag, or water-soluble silver sources, with UO_3 and I_2O_5 at 200 °C for 5 days yields $Ag_4(UO_2)_4(IO_3)_2(IO_4)_2O_2$ in the form of orange fibrous needles. Single-crystal X-ray diffraction studies on this compound reveal a highly complex network structure consisting of three interconnected low-dimensional substructures. The first of these substructures are ribbons of UO_8 hexagonal bipyramids that edge-share to form one-dimensional chains. These units further edge-share with pentagonal bipyramidal UO_7 units to create ribbons. The edges of the ribbons are partially terminated by tetraoxoiodate(V), $[IO_4]^{3-}$, anions. The uranium oxide ribbons are joined by bridging iodate ligands to yield two-dimensional undulating sheets. These sheets help to form, and are linked together by, one-dimensional chains of edge-sharing AgO_7 capped octahedral units and ribbons formed by corner-sharing capped trigonal planar AgO_4 polyhedra, AgO_6 capped square pyramids, and AgO_6 octahedra. The $[IO_4]^{3-}$ anions in $Ag_4(UO_2)_4(IO_3)_2(IO_4)_2O_2$ are tetraoxoiodate(V), not metaperiodate, and contain I(V) with a stereochemically active lone-pair. Bond valence sum calculations are consistent with this formulation. Differential scanning calorimetry measurements show distinctly different thermal behavior of $Ag_4(UO_2)_4(IO_3)_2(IO_4)_2O_2$ versus other uranyl iodate compounds with endotherms at 479 and 494 °C. Density functional theory (DFT) calculations demonstrate that the approximate C_{2v} geometry of the $[IO_4]^{3-}$ anion can be attributed to a second-order Jahn−Teller distortion. DFT optimized geometry for the $[IO_4]^{3-}$ anion is in good agreement with those measured from single-crystal X-ray diffraction studies on $Ag_4(UO_2)_4(IO_3)_2(IO_4)_2O_2$.

Introduction

Oxoanions of iodine display highly complex chemistry in both solution and the solid state owing to a series of equilibria among periodate, $[IO_6]$,$^{5-}$ and metaperiodate, $[IO_4]^-$, species in aqueous media[1] and the thermal disproportionation of iodate to metaperiodate and iodine at moderate to high temperatures in the solid state.[2−6] As ligands, iodate and periodate display a number of unusual properties. The former anion, having C_{3v} symmetry and a stereochemically active lone-pair, has a propensity for yielding compounds with low-dimensional character.[7,8] Furthermore, these solids often crystallize in noncentrosymmetric space groups, especially with lanthanides, and therefore have been the subject of considerable physicochemical property measurements.[9−13] The latter anion has the ability to stabilize unusually high oxidation states for transition metals, including Cu(III),[14−16] Ag(III),[14,15,17] and Ni(IV).[18]

Our recent efforts in the preparation of new solids containing oxoanions of iodine has focused on the hydrothermal syntheses of low-dimensional uranyl iodates.[7,8] The straightforward reaction of UO_3 with I_2O_5 yields $UO_2(IO_3)_2(H_2O)$ or $UO_2(IO_3)_2$ depending on whether mild (<250 °C) or supercritical (>374 °C) temperatures are employed.[7] However, the uranyl iodate framework is quite versatile, and a large number of cations can be incorporated to yield new compounds, including alkali metals, alkaline-earth metals, and main group elements. This has allowed for the isolation and structural elucidation of $A_2[(UO_2)_3(IO_3)_4O_2]$ (A = K,[7] Rb[19], Tl[19]), $Cs_2[(UO_2)_3Cl_2(IO_3)(OH)O_2]\cdot 2H_2O$, and $AE[(UO_2)_2(IO_3)_2O_2](H_2O)$ (AE = Sr,[19] Ba,[7] Pb[19]).

[†] Auburn University.
[‡] Bruker AXS.

(1) Buist, G. J.; Hipperson, W. C. P.; Lewis, J. D. *J. Chem. Soc. A* **1969**, *2*, 307.
(2) Alici, E.; Schmidt, T.; Lutz, H. D. *Z. Anorg. Allg. Chem.* **1992**, *608*, 135.
(3) Hoppe, R.; Schneider, J. *J. Less-Common Met.* **1988**, *137*, 85.
(4) Hejek, B.; Hradilova, J. *J. Less-Common Met.* **1971**, *23*, 217.
(5) Nassau, K.; Shiever, J. W.; Prescott, B. E.; Cooper, A. S. *J. Solid State Chem.* **1974**, *11*, 314.
(6) Nassau, K.; Shiever, J. W.; Prescott, B. E. *J. Solid State Chem.* **1975**, *14*, 122.
(7) Bean, A. C.; Peper, S. M.; Albrecht-Schmitt, T. E. *Chem. Mater.* **2001**, *13*, 1266.
(8) Bean, A. C.; Ruf, M.; Albrecht-Schmitt, T. E. *Inorg. Chem.* **2001**, *40*, 3959.
(9) Liminga, R.; Abrahams, S. C.; Bernstein, J. L. *J. Chem. Phys.* **1975**, *62*, 755.
(10) Abrahams, S. C.; Bernstein, J. L.; Nassau, K. *J. Solid State Chem.* **1976**, *16*, 173.
(11) Abrahams, S. C.; Bernstein, J. L.; Nassau, K. *J. Solid State Chem.* **1977**, *22*, 243.
(12) Abrahams, S. C.; Bernstein, J. L. *J. Chem. Phys.* **1978**, *69*, 2505.
(13) Gupta, P. K.; Ammon, H. L.; Abrahams, S. C. *Acta Crystallogr.* **1989**, *C45*, 175.
(14) Dengel, A. C.; Elhendawy, A. M.; Griffith, W. P.; Mostafa, S. I.; Williams, D. J. *J. Chem. Soc., Dalton Trans.* **1992**, *24*, 3489.
(15) Balikungeri, A.; Pelletier, M.; Monnier, D. *Inorg. Chim. Acta* **1977**, *22*, 7.
(16) Masse, R.; Durif, A. *J. Solid State Chem.* **1988**, *73*, 206.
(17) Adelskoeld, V.; Eriksson, L.; Wang, P. L.; Werner, P. E. *Acta Crystallogr.* **1988**, *C44*, 597.
(18) Currie, D. B.; Levason, W.; Oldroyd, R. D.; Weller, M. T. *J. Chem. Soc., Dalton Trans.* **1994**, *9*, 1483.
(19) Bean, A. C.; Albrecht-Schmitt, T. E. *J. Solid State Chem.* **2001**, *submitted*.

10.1021/ja011204y CCC: $20.00
Published on Web 08/15/2001

The ability of the uranyl iodate networks to accommodate such a wide variety of counterions is based on two key structural features of this system. First, the uranyl cation can adopt a wide variety of coordination environments ranging from six-coordinate $[UO_2X_4]^{n-}$ square bipyramids, to seven-coordinate $[UO_2X_5]^{n-}$ pentagonal bipyramids, to eight-coordinate $[UO_2X_6]^{n-}$ hexagonal bipyramids.[20,21] This feature has been capitalized upon in the development of a large series of low-dimensional and open-framework uranyl oxyfluorides,[22−27] phosphates,[28] and molybdates.[29] Second, the iodate ligand can participate in at least five different binding modes including the bridging of two or three metal centers,[7,8,30] the chelation of a single metal,[7] chelation and simultaneous bridging by an oxygen atom of the iodate adopting μ_3 ligation,[7] and finally monodentate coordination.[8]

During our exploration of the preparation of new transition metal uranyl iodates, we discovered that the hydrothermal reaction of elemental silver or water-soluble silver sources, such as silver nitrate, with UO_3 and I_2O_5 produces $Ag_4(UO_2)_4(IO_3)_2(IO_4)_2O_2$ in the form of fibrous orange needles. At first glance, this compound appears to be a mixed-valent iodine compound containing both iodate and metaperiodate. However, the $[IO_4]$ units are actually tetraoxoiodate(V), $[IO_4]^{3-}$, and the structural results clearly demonstrate the influence of a stereochemically active lone-pair on this anion. This is the first report of this new oxoanion. The details on the preparation and characterization of $Ag_4(UO_2)_4(IO_3)_2(IO_4)_2O_2$ are reported herein.

Experimental Section

Syntheses. Ag (99.99%, Stern-Leach), UO_3 (99.8%, Alfa-Aesar), and I_2O_5 (98%, Alfa-Aesar) were used as received. Distilled and Millipore filtered water was used in all reactions. The resistance of the water was 18.2 MOhm. *While the UO_3 contains depleted U, standard precautions for handling radioactive materials should be followed.* SEM/EDX analyses were performed using a JEOL 840/Link Isis instrument. Silver, uranium, and iodine standards were used to calibrate results, and EDX ratios are within 3% of the ratios determined from single-crystal X-ray diffraction experiments.

$Ag_4(UO_2)_4(IO_3)_2(IO_4)_2O_2$. Ag (300 mg, 2.78 mmol), UO_3 (429 mg, 1.5 mmol), and I_2O_5 (334 mg, 1 mmol) were loaded in a 23-mL PTFE-lined autoclave. Water (1 mL) was then added to the solids. The autoclave was sealed and placed in a box furnace and heated to 200 °C. After 5 days the furnace was cooled at 9 °C/h to 23 °C. The product consisted of bundles of orange fibrous needles of $Ag_4(UO_2)_4(IO_3)_2(IO_4)_2O_2$ and bright yellow truncated tetragonal bipyramids of $UO_2(IO_3)_2(H_2O)$. The mother liquor was decanted from the crystals, which were then washed with water and methanol and allowed to dry. Yield, 376 mg (44% yield based on U). EDX analysis: Ag, 34.10%, U, 35.54%; I, 30.36%. IR (KBr, cm^{-1}): ν(U=O) 927 (w); ν(U=O, U−O, Ag−O, and I=O) 843 (s), 835 (s), 812 (m), 788 (m), 772 (m), 756 (m), 728 (s), 714 (s, sh), 668 (w), 640 (m), 628 (m), 614 (m), 597 (w, sh), 585 (w, sh), 567 (w, sh), 555 (w), 542 (w, sh), 502 (w, sh), 460 (s, sh), 445 (s), 433 (s, sh). DSC thermogram endotherms: 479 (−1.624 W/g), 494 °C (−1.480 W/g).

Table 1. Crystallographic Data for $Ag_4(UO_2)_4(IO_3)_2(IO_4)_2O_2$

formula	$Ag_4(UO_2)_4(IO_3)_2(IO_4)_2O_2$
formula mass (amu)	2275.20
space group	$P2_1/n$ (No. 14)
a (Å)	15.040(7)
b (Å)	8.051(4)
c (Å)	18.332(8)
α (deg)	90
β (deg)	100.738(7)
γ (deg)	90
V (Å^3)	2181(2)
Z	4
T (°C)	22
2θ range (deg)	3.22−46.62
λ (Å)	0.710 73
ρ_{calcd} (g cm^{-3})	6.929
μ(Mo Kα) (cm^{-1})	388.69
goodness-of-fit, all data	1.042
largest difference peak and hole (eÅ^3)	2.777 and −1.763
$R(F)$ for $F_o^2 > 2\sigma(F_o^2)$[a]	0.0514
$R_w(F_o^2)$[b]	0.1077

[a] $R(F) = \{\sum||F_o| - |F_c||\}/\{\sum|F_o|\}$. [b] $R_w(F_o^2) = [\{\sum[w(F_o^2 - F_c^2)^2]\}/\{\sum wF_o^4\}]^{1/2}$.

Crystallographic Studies. An orange fibrous needle of $Ag_4(UO_2)_4(IO_3)_2(IO_4)_2O_2$ (∼0.004 × ∼0.004 × 0.410 mm) was mounted on a glass fiber and aligned on a Bruker SMART APEX CCD X-ray diffractometer. Intensity measurements were performed using graphite monochromated Mo Kα radiation from a sealed tube and a monocapillary. SMART was used for preliminary determination of the cell constants and data collection control. The intensities of reflections of a sphere were collected by a combination of 3 sets of exposures (frames). Each set had a different ϕ angle for the crystal and each exposure covered a range of 0.3° in ω. A total of 1800 frames were collected with an exposure time per frame of 120 s. The long exposure time was necessary owing to the extremely thin nature of these crystals and correspondingly weak diffraction.

The determination of integral intensities and global cell refinement were performed with the Bruker SAINT (v 6.02) software package using a narrow-frame integration algorithm. A semiempirical absorption correction was applied based on the intensities of symmetry-related reflections measured at different angular settings using SADABS.[31] The program suite SHELXTL (v 5.1) was used for space group determination (XPREP), structure solution (XS), and refinement (XL).[32] The final refinement included anisotropic displacement parameters for Ag, U, and I atoms. The oxygen atoms were refined isotropically. Ag and I atoms can be distinguished on the basis of both thermal parameters and Ag−O versus I−O bond distances. Some crystallographic details are listed in Table 1, additional details can be found in the Supporting Information. Two other complete datasets on different crystals of $Ag_4(UO_2)_4(IO_3)_2(IO_4)_2O_2$, including low-temperature data, were collected and the structures were solved. These refinements are consistent with the structure reported herein.

Thermal Analysis. Thermal data for $Ag_4(UO_2)_4(IO_3)_2(IO_4)_2O_2$ were collected using a TA Instruments, Model 2920 Differential Scanning Calorimeter (DSC). Samples (20 mg) were encapsulated in aluminum pans and heated at 10 °C/min from 25 to 600 °C under a nitrogen atmosphere.

(20) Burns, P. C.; Ewing, R. C.; Hawthorne, F. C. *Can. Mineral.* **1997**, *35*, 1551.
(21) Burns, P. C.; Miller, M. L.; Ewing, R. C. *Can. Mineral.* **1996**, *34*, 845.
(22) Almond, P. M.; Talley, C. E.; Bean, A. C.; Peper, S. M.; Albrecht-Schmitt; T. E. *J. Solid State Chem.* **2000**, *154*, 635.
(23) Talley, C. E.; Bean, A. C.; Albrecht-Schmitt, T. E. *Inorg. Chem.* **2000**, *39*, 5174.
(24) Allen, S.; Barlow, S.; Halasyamani, P. S.; Mosselmans, J. F. W.; O'Hare, D.; Walker, S. M.; Walton, R. I. *Inorg. Chem.* **2000**, *39*, 3791.
(25) Halasyamani, P. S.; Walker, S. M.; O'Hare, D. *J. Am. Chem. Soc.* **1999**, *121*, 7415.
(26) Walker, S. M.; Halasyamani, P. S.; Allen, S.; O'Hare, D. *J. Am. Chem. Soc.* **1999**, *121*, 10513.
(27) Francis, R. J.; Halasyamani, P. S.; Bee, J. S.; O'Hare, D. *J. Am. Chem. Soc.* **1999**, *121*, 1609.
(28) Francis, R. J.; Drewitt, M. J.; Halasyamani, P. S.; Ranganathachar, C.; O'Hare, D.; Clegg, W.; Teat, S. J. *Chem. Commun.* **1998**, *2*, 279.
(29) Halasyamani, P. C.; Francis, R. J.; Walker, S. M.; O'Hare, D. *Inorg. Chem.* **1999**, *38*, 271.
(30) Weigel, F.; Engelhardt, L. W. H. *J. Less-Common Met.* **1983**, *91*, 339.
(31) *SADABS*, Program for absorption correction using SMART CCD based on the method of Blessing: Blessing, R. H. *Acta Crystallogr.* **1995**, *A51*, 33.
(32) Sheldrick, G. M. *SHELXTL PC*, Version 5.0, An Integrated System for Solving, Refining, and Displaying Crystal Structures from Diffraction Data; Siemens Analytical X-Ray Instruments, Inc.: Madison, WI, 1994.

Results and Discussion

Syntheses. The reaction of Ag with UO_3 and I_2O_5 in aqueous media at 200 °C for 5 days under autogenously generated pressure results in the formation of $Ag_4(UO_2)_4(IO_3)_2(IO_4)_2O_2$ in 44% yield. This compound can also be synthesized from the reaction of $AgNO_3$ with UO_3 and I_2O_5 or HIO_3. Lowering the reaction temperature to 180 °C, or increasing the temperature to 425 °C (supercritical), does not result in a change in product composition with the exception of the transformation of the $UO_2(IO_3)_2(H_2O)$ byproduct to $UO_2(IO_3)_2$.[7] Furthermore, decreasing the reaction duration to 1 day or increasing the duration to 5 days also has little effect on product composition. We explored this wide variety of experimental conditions and starting materials in an effort to increase the size of the crystals of $Ag_4(UO_2)_4(IO_3)_2(IO_4)_2O_2$, which only form very thin, fibrous, orange needles. The observation that this compound always forms in these reactions, regardless of experimental conditions, implies that it is probably remarkably insoluble, and once formed, precipitates rapidly. The reported synthesis produced the largest crystals that we have been able to grow.

Clearly, UO_3 and I_2O_5 are highly oxidizing, as silver tubing is often used to contain hydrothermal reactions as an inert vessel.[33] However, we have yet to observe the oxidation of iodate to periodate or metaperiodate in these reactions. Surprisingly, reactions performed using H_5IO_6 also yield iodate compounds. $Ag_4(UO_2)_4(IO_3)_2(IO_4)_2O_2$ shows dramatically different thermal behavior than other uranyl iodate compounds, which thermally disproportionate at approximately 570 °C.[7,8] This compound, however, shows two endotherms of approximately equal area at 479 and 494 °C that most likely correspond to the disproportionation of the tetraoxoiodate(V) and iodate ligands through loss of I_2.

Structure of $Ag_4(UO_2)_4(IO_3)_2(IO_4)_2O_2$. The structure of $Ag_4(UO_2)_4(IO_3)_2(IO_4)_2O_2$ is a highly complex network consisting of three interconnected substructures. The first of these are one-dimensional uranium oxide ribbons consisting of both UO_8 hexagonal bipyramids and UO_7 pentagonal bipyramids. The UO_8 units edge-share to form one-dimensional chains that further share edges with UO_7 units to yield one-dimensional ribbons. The edges of these ribbons are partially terminated by tetraoxoiodate(V), $[IO_4]^{3-}$, anions (vide infra). A polyhedral representation of part of one of these ribbons is depicted in Figure 1. The coordination sphere of the UO_7 units is completed, in part, through ligation by iodate anions. These iodate groups bridge between the one-dimensional uranium oxide ribbons to create undulating two-dimensional $^2_\infty[(UO_2)_4(IO_3)_2(IO_4)_2O_2]^{4-}$ sheets that run down the *b*-axis as shown in Figure 2. U−O and U═O bonds range from 2.17(2) to 2.63(2) Å and from 1.77(2) to 1.85(2) Å, respectively. The long U−O bonds are due to ligation by the iodate and tetraoxoiodate ligands. Similar bond lengthening has been observed in other uranyl iodate compounds.[7,8] Shorter U−O bonds are with the μ_3 oxide ligands present in the ribbons.

The oxygen atoms of the uranyl units and the iodate oxygen atoms not involved in bonding with the uranium atoms form two distinct silver oxide networks. The first of these, shown in Figure 3a, consists of capped octahedral AgO_7 units that edge-share with one another to form one-dimensional chains. Ag−O bond distances show significant variation ranging from 2.39(2) to 2.70(2) Å. The second silver oxide network is formed from the corner-sharing of capped trigonal planar AgO_4 polyhedra, AgO_6 capped square pyramids, and AgO_6 octahedra. Part of one of these ribbons is shown in Figure 3b. Again significant variations in Ag−O bond lengths are found with bond distances of 2.25(2) to 2.51(2) Å, 2.39(2) to 2.66(2) Å, and 2.38(2) to 2.71(2) Å being found for Ag(2), Ag(3), and Ag(4), respectively. Both of these one-dimensional Ag−O systems run down the *b*-axis parallel with the uranium oxide chains. When the silver oxide substructures are combined with the uranium oxide sheets the highly complex three-dimensional network structure depicted

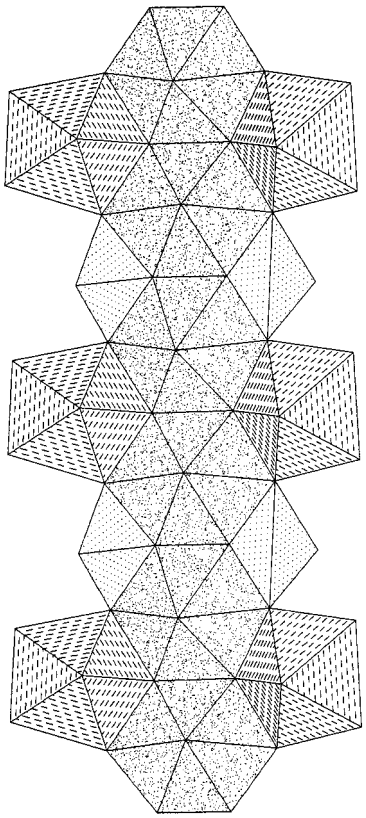

Figure 1. A polyhedral representation of the uranium oxide ribbons formed from UO_8 hexagonal bipyramids and UO_7 pentagonal bipyramids in $Ag_4(UO_2)_4(IO_3)_2(IO_4)_2O_2$.

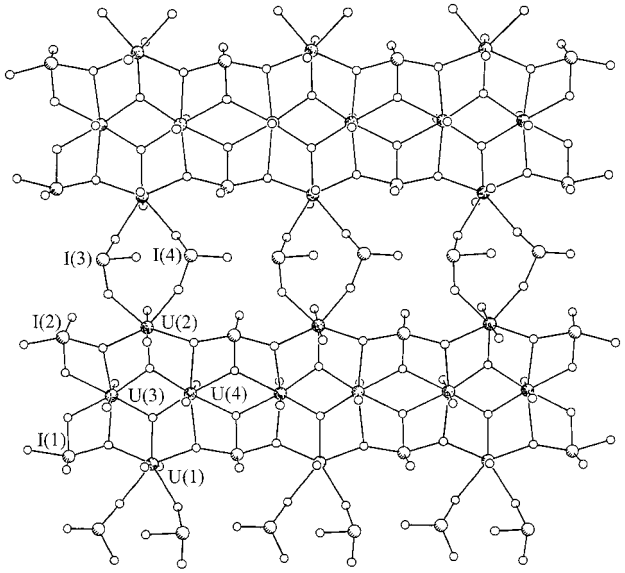

Figure 2. Two-dimensional $^2_\infty[(UO_2)_4(IO_3)_2(IO_4)_2O_2]^{4-}$ undulating sheets that run down the *b*-axis in $Ag_4(UO_2)_4(IO_3)_2(IO_4)_2O_2$. These sheets are created by iodate ligands bridging between one-dimensional uranium oxide ribbons.

(33) Kolis, J. W.; Korzenski, M. B. In *Chemical Synthesis Using Supercritical Fluids*; Jessop, P. G., Leitner, W., Eds.; Wiley-VCH: New York, 1999; p 213.

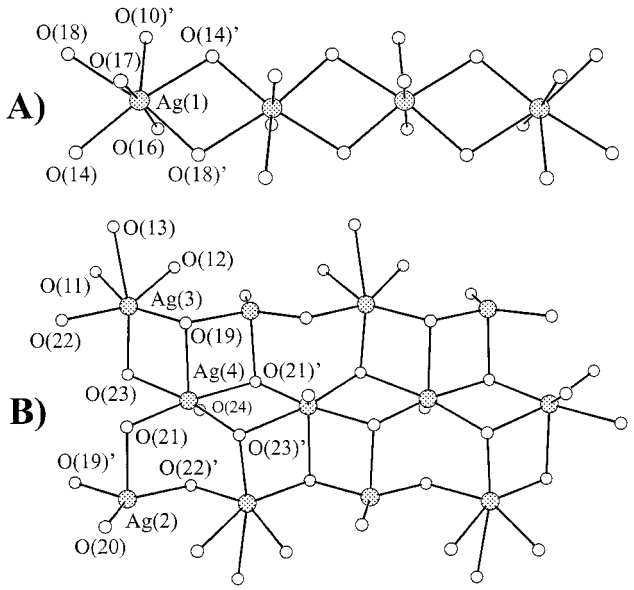

Figure 3. (a) Capped octahedral AgO_7 units that edge-share with one another to form one-dimensional chains in $Ag_4(UO_2)_4(IO_3)_2(IO_4)_2O_2$. (b) A second silver oxide network formed from the corner-sharing of capped trigonal planar AgO_4 polyhedra, AgO_6 capped square pyramids, and AgO_6 octahedra.

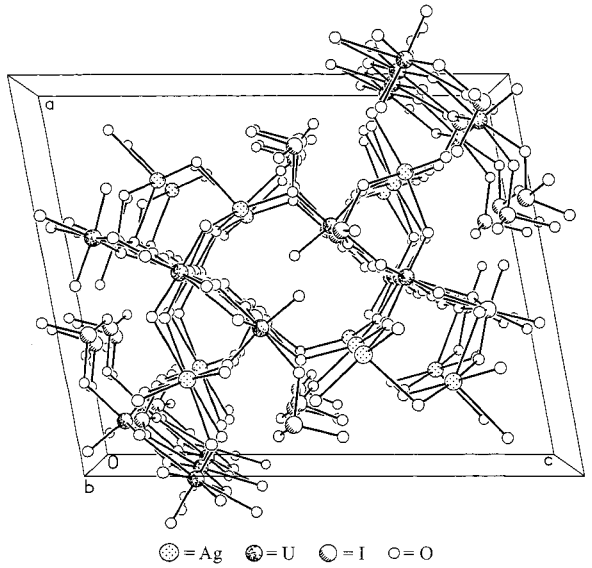

Figure 4. A view of the interconnection of the silver oxide and uranium oxide substructures in the unit cell of $Ag_4(UO_2)_4(IO_3)_2(IO_4)_2O_2$.

in Figure 4 is created. The polyhedra described in this section are done so using a maximum Ag−O distance of 3.0 Å.

Finally we come to the key feature of this structure, the tetraoxoiodate(V), $[IO_4]^{3-}$, anion. There are two crystallographically unique $[IO_4]^{3-}$ anions in $Ag_4(UO_2)_4(IO_3)_2(IO_4)_2O_2$. Both of these have approximate C_{2v} symmetry with four oxygen atoms bent away from a tetrahedral coordination into a seesaw geometry. These anions are depicted in Figure 5. I(1)−O bonds to O(3), O(4), O(10), and O(18) are 1.82(2), 1.88(2), 1.97(2), and 1.97(2) Å, respectively. The observed compression of the O(3)−I(1)−O(10) and O(4)−I(1)−O(18) bond angles of 154.3(7)° and 105.1(7)°, respectively, indicates the presence of a lone-pair. I(2)−O bonds to O(5), O(6), O(21), and O(24) are 1.82(2), 1.83(2), 1.98(2), and 1.99(2) Å, and are similar to those found with I(1) as there are two short and two long I−O bonds. The $[IO_4]^{3-}$ anion containing I(2) also displays compression of O−I−O bond angles with O(6)−I(2)−O(24) and O(5)−I(2)−

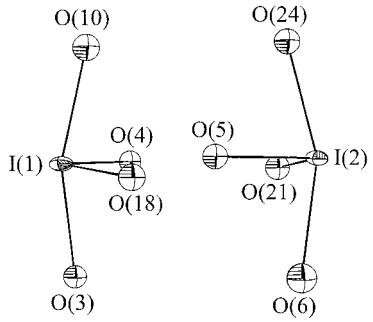

Figure 5. A view of both approximately C_{2v} tetraoxoiodate(V), $[IO_4]^{3-}$, anions in $Ag_4(UO_2)_4(IO_3)_2(IO_4)_2O_2$. Fifty percent anisotropic ellipsoids are depicted for the iodine atoms. The oxygen atoms have been refined isotropically.

Table 2. I−O Bond Distances (Å) in Tetraoxoiodate(V), $[IO_4]^{3-}$, and Iodate Anions for $Ag_4(UO_2)_4(IO_3)_2(IO_4)_2O_2$

I−O distances in tetraoxoiodate(V), $[IO_4]^{3-}$			
I(1)−O(3)	1.97(2)	I(2)−O(5)	1.83(2)
I(1)−O(4)	1.88(2)	I(2)−O(6)	1.99(2)
I(1)−O(10)	1.97(2)	I(2)−O(21)	1.82(2)
I(1)−O(18)	1.82(2)	I(2)−O(24)	1.98(2)
I−O distances in iodate, $[IO_3]^-$			
I(3)−O(7)	1.78(2)	I(4)−O(8)	1.81(2)
I(3)−O(11)	1.84(2)	I(4)−O(12)	1.83(2)
I(3)−O(15)	1.79(2)	I(4)−O(20)	1.79(2)

O(21) angles of 153.9(7)° and 99.7(7)°. The differences in the geometry of these tetraoxoiodate(V) anions are due to differences in coordination to surrounding metal centers. While both anions bridge uranium centers with three μ_3 oxygen atoms from each tetraoxoiodate(V) unit, the remaining oxygen atoms coordinate silver cations above and beneath the layers. Herein lies the difference between the two anions. The O(21) atom from I(2) forms three contacts with silver centers, whereas the O(18) atom from I(2) only forms two such contacts. The remaining iodate anions show normal bond distances and angles. I−O bond distances for both $[IO_4]^{3-}$ and $[IO_3]^-$ are listed in Table 2.

The central question here is how did this new ligand form? The answer to this question may lie in the structures of other uranyl iodate compounds that contain one-dimensional uranium oxide chains with their edges terminated by iodate ligands. $K_2[(UO_2)_3(IO_3)_4O_2]$ and $Ba[(UO_2)_2(IO_3)_2O_2](H_2O)$ both contain such chains where the chain edges are terminated by bridging and monodentate iodate ligands.[8] In these compounds there are close I···O contacts ranging from 2.397(3) to 2.667(9) Å between the terminal oxygen atoms from the monodentate iodate ligand and the neighboring iodine atom from the iodate that bridges uranium centers.[8] These types of interactions are very common in the structures of iodate compounds in general. If these close I···O contacts were to actually lead to a full oxygen atom transfer, then a $[IO_4]^{3-}$ anion would result. This may in fact be the mechanism by which iodate thermally disproportionates to metaperiodate, IO_4^-, and I_2, with $Ag_4(UO_2)_4(IO_3)_2(IO_4)_2O_2$ representing a trapped intermediate in this process.[34]

Bond Valence Sum Calculations. There are several key concerns about the identity of $Ag_4(UO_2)_4(IO_3)_2(IO_4)_2O_2$ that can be alleviated through bond valence sum calculations.[35,36] Our first concern was that the tetraoxoiodate(V) units did not contain pentavalent iodine, but rather heptavalent iodine. However, the

(34) Gorski, A.; Milczarek, M. *Pol. J. Chem.* **1984**, *58*, 635.
(35) Brown, I. D.; Altermatt, D. *Acta Crystallogr.* **1985**, *B41*, 244.
(36) Brese, N. E.; O'Keeffe, M. *Acta Crystallogr.* **1991**, *B47*, 192.

Table 3. Bond Valence Sums for the Silver, Uranium, and Iodine Centers in $Ag_4(UO_2)_4(IO_3)_2(IO_4)_2O_2$

Ag(1)	0.848	Ag(3)	0.884
Ag(2)	0.862	Ag(4)	0.829
U(1)	6.231	U(3)	6.065
U(2)	5.999	U(4)	6.049
I(1)	5.187	I(2)	5.301
I(3)	5.140	I(4)	5.022

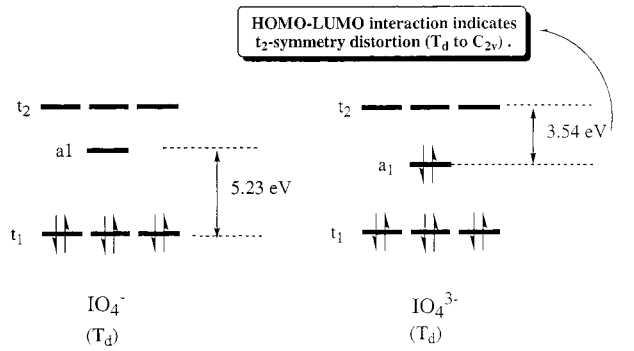

Figure 6. The stabilizing distortion ($T_d \rightarrow C_{2v}$) of the tetraoxoiodate-(V), $[IO_4]^{3-}$, anion, which lowers the energy by 7.9 kcal/mol with zero-point correction, can be attributed to a second-order Jahn−Teller (SOJT) interaction between the HOMO (a_1) and LUMO (t_2).

bond valence sums for I(1) and I(2) are 5.187 and 5.301, respectively. These values compare well with those obtained for I(3) and I(4), which are present in the iodate anions, and have values of 5.140 and 5.022, respectively. These are also in the same range of values found for the iodine atoms in all other uranyl iodate compounds.[7,8] Our second concern was the possibility of having a mixed-valent uranium compound. However, U(1), U(2), U(3), and U(4) have bond valence sums that range from 5.999 to 6.231.[20] Finally, our third concern was that we might have a Ag(III) compound, as the periodate ligand can stabilize such oxidation states.[14,15,17] This final concern can be discounted as Ag(1), Ag(2), Ag(3), and Ag(4) have bond valence values that all occur between 0.829 and 0.884. Bond valence sums are listed in Table 3.

Electronic Structure of $[IO_4]^{3-}$. Theoretical calculations were carried out using the Gaussian 98 program[37] to understand the electronic structure of the $[IO_4]^{3-}$ anion. $[IO_4]^{3-}$ was optimized with the B3LYP level[38] of density functional theory (DFT).[39] The quasirelativistic Stuttgart/Dresden effective core potential[40] was applied to iodine with a (31/31/1) contraction for the valence electrons[41] and the 6-31G(d) basis set[42] was applied to oxygen. A C_{2v}-symmetry structure was characterized as the global minimum on the $[IO_4]^{3-}$ potential energy surface by frequency calculations, while the T_d-symmetry structure had three imaginary frequencies (t_2-symmetry mode). The three transition vectors of the T_d-optimized geometry (animated by Molden[43]) indicate a distortion to C_{2v} geometry. As illustrated in Figure 6, the stabilizing distortion ($T_d \rightarrow C_{2v}$), which lowers the energy by 7.9 kcal/mol with zero-point correction, can be attributed to a second-order Jahn−Teller (SOJT) interaction[44] between the HOMO (a_1) and LUMO (t_2). SOJT distortions also play an important role in the geometries of other ions with stereochemically active lone-pairs such as Se(IV), Te(IV), and Pb(II).[45]

DFT optimized geometry for the $[IO_4]^{3-}$ anion is in good agreement with those measured from single-crystal X-ray diffraction studies on $Ag_4(UO_2)_4(IO_3)_2(IO_4)_2O_2$. These calculations provide two long and two short I−O bond lengths of 2.059 and 1.935 Å. These values compare well with measured average I−O bond lengths of 1.98(2) and 1.84(2) Å that also show two long and two short I−O bonds around each iodine atom. More importantly, the average measured O−I−O bond angles of 154.1(7)° and 102.4(7)° conform remarkably well to the calculated bond angles of 158.7° and 101.8°.

Conclusions

In this report we have described the first example of a new fundamental oxoanion of iodine, namely tetraoxoiodate(V). This anion may represent a structural intermediate or perhaps a model of the pathway by which iodate thermally disproportionates to metaperiodate and iodine. In future studies we will address whether tetraoxoiodate(V) has an existence independent of $Ag_4(UO_2)_4(IO_3)_2(IO_4)_2O_2$.

Acknowledgment. This work was supported by NASA (Alabama Space Grant Consortium) and Auburn University.

Supporting Information Available: X-ray crystallographic files for $Ag_4(UO_2)_4(IO_3)_2(IO_4)_2O_2$ (CIF). This material is available free of charge via the Internet at http://pubs.acs.org.

JA011204Y

(37) Frisch, M. J.; Trucks, G. W.; Schlegel, H. B.; Scuseria, G. E.; Robb, M. A.; Cheeseman, J. R.; Zakrzewski, V. G.; Montgomery, J. A., Jr.; Stratmann, R. E.; Burant, J. C.; Dapprich, S.; Millam, J. M.; Daniels, A. D.; Kudin, K. N.; Strain, M. C.; Farkas, O.; Tomasi, J.; Barone, V.; Cossi, M.; Cammi, R.; Mennucci, B.; Pomelli, C.; Adamo, C.; Clifford, S.; Ochterski, J.; Petersson, G. A.; Ayala, P. Y.; Cui, Q.; Morokuma, K.; Malick, D. K.; Rabuck, A. D.; Raghavachari, K.; Foresman, J. B.; Cioslowski, J.; Ortiz, J. V.; Stefanov, B. B.; Liu, G.; Liashenko, A.; Piskorz, P.; Komaromi, I.; Gomperts, R.; Martin, R. L.; Fox, D. J.; Keith, T.; Al-Laham, M. A.; Peng, C. Y.; Nanayakkara, A.; Gonzalez, C.; Challacombe, M.; Gill, P. M. W.; Johnson, B. G.; Chen, W.; Wong, M. W.; Andres, J. L.; Head-Gordon, M.; Replogle, E. S.; Pople, J. A. *Gaussian 98*, revision *A.7*; Gaussian, Inc.: Pittsburgh, PA, 1998.

(38) Becke, A. D. *J. Chem. Phys*. **1993**, *98*, 5648.

(39) Parr, R. G.; Yang, W. *Density-Functional Theory of Atoms and Molecules*; Oxford University Press: Oxford, 1989.

(40) (a) Bergner, A.; Dolg, M.; Küchle, W.; Stoll, H.; Preuss, H. *Mol. Phys.* **1993**, *80*, 1431. (b) Schwerdtfeger, P.; Dolg, M.; Schwarz, W. H.; Bowmaker, G. A.; Boyd, P. D. W. *J. Chem. Phys*. **1989**, *91*, 1762.

(41) Glukhovtsev, N. M.; Pross, A.; McGrath, M. P.; Radom, L. *J. Chem. Phys*. **1995**, *103*, 1878. Erratum: *J. Chem. Phys*. **1996**, *104*, 3407.

(42) (a) Hehre, W. J.; Radom, L.; Schleyer, P. v. R.; Pople, J. A. *Ab Initio Molecular Orbital Theory*; Wiley: New York, 1986. (b) Jensen, F. *Introduction to Computational Chemistry*; Wiley: New York, 1999.

(43) MOLDEN: Schaftenaar, G.; Noordik, J. H. Molden: a pre- and post-processing program for molecular and electronic structures: *J. Comput.-Aided Mol. Design* **2000**, *14*, 123−134.

(44) The direction of the second-order Jahn−Teller (SOJT) distortion in the IO_4^{3-} trianion is given by a direct product ($a_1 \times t_2 = t_2$) of orbital symmetries of HOMO (a_1) and LUMO (t_2): Pearson, R. G. *Theochem* **1983**, *12*, 25.

(45) (a) Halasyamani, P. S.; Poeppelmeier, K. R. *Chem. Mater*. **1998**, *10*, 2753. (b) Ok, K. M.; Bhuvanesh, N. S. P.; Halasyamani, P. S. *Inorg. Chem.* **2001**, *40*, 1978.